Dynamics of a Flexible Loop in Dihydrofolate Reductase from *Escherichia coli* and Its Implication for Catalysis†

Christopher J. Falzone,‡ Peter E. Wright,§ and Stephen J. Benkovic*,‡

Department of Chemistry, 152 Davey Laboratory, The Pennsylvania State University, University Park, Pennsylvania 16802, and Department of Molecular Biology, The Scripps Research Institute, 10666 North Torrey Pines Road, La Jolla, California 92037

Received September 17, 1993; Revised Manuscript Received October 12, 1993®

ABSTRACT: Apo-dihydrofolate reductase from *Escherichia coli* samples two distinct environments slowly on the NMR time scale at room temperature. Several assigned resonances belong to residues in, or proximal to, a loop (loop I) which is comprised of residues 9–24. This exchange process was altered (either removed or made fast on the NMR time scale) by deleting three hairpin turn forming residues from the loop and filling the gap with a single glycine [Li, L., Falzone, C. J., Wright, P. E., & Benkovic, S. J. (1992) *Biochemistry 31*, 7826–7833]. An approximate value of 35 s^{-1} for the exchange rate associated with loop I in apo-DHFR was obtained in two-dimensional nuclear Overhauser spectra by analyzing the time dependence of the cross-peak volume for $N^{\epsilon}H$ of Trp-22, a residue which is located in this loop and which has resolved cross-peaks. Owing to the critical role that this loop plays in catalysis, the correspondence between this rate of conformational exchange and off-rates for tetrahydrofolate and the reduced nicotinamide cofactor from product and substrate complexes suggests that loop movement may be a limiting factor in substrate turnover.

Dihydrofolate reductase (DHFR)[1] (5,6,7,8-tetrahydrofolate:$NADP^+$ oxidoreductase, EC 1.5.1.3) catalyzes the NADPH-dependent reduction of 7,8-dihydrofolate (H_2F) to 5,6,7,8-tetrahydrofolate (H_4F). It is a monomeric protein consisting of 159 residues, and in its apo form, it displays at least 2 separate conformational equilibria as detected by two-dimensional NMR methods (Falzone et al., 1991; Li et al., 1992). One is very slow [k_{iso} = 0.03 s^{-1} as measured by fluorescence (Cayley et al., 1981; Fierke et al., 1987)] and in the case of the methotrexate (MTX) binary complex gives rise to doubled cross-peaks for residues located primarily within the eight-stranded β-sheet. These two isomers were identified with the E_1/E_2 isomers (Falzone et al., 1991) first described by Cayley et al. (1981) which represent two forms of DHFR with very different affinities for substrates: E_1 readily binds both NADPH and H_2F whereas E_2 binds only NADPH but with a K_D that is higher by 100-fold (Adams et al., 1989; Appleman et al., 1990). The second dynamic process was proposed to involve residues associated with loop I (Ala-9–Leu-24) (Li et al., 1992). A portion of loop I (residues 16–20) was observed to be disordered in the X-ray crystal structure of the apoprotein (Bystroff & Kraut, 1991). This loop encapsulates the ternary complex of $NADP^+$ and folate and allows the protein to recruit hydrophobic residues to the active site after substrate binding (Bystroff et al., 1990). The motions of this loop may be coupled to catalysis (Li et al., 1992; Farnum et al., 1991).

A molecular interpretation has been proposed for the role of loop I. Met-20, which makes van der Waals contact with $NADP^+$ in the ternary complex (Bystroff et al., 1990), may stabilize the transition state (Li et al., 1992; Farnum et al., 1991) possibly through confinement of the reacting molecules (Bystroff et al., 1990) or by selection of a reactive substrate conformation (Hershlag, 1988). When the residues of loop I which form a hairpin turn (16–19) are replaced by a single glycine, a 500-fold reduction in the rate of hydride transfer from NADPH to dihydrofolate is observed, thus highlighting the importance of this loop in catalysis (Li et al., 1992). Taking advantage of the slow exchange (on the chemical shift time scale) of residues associated with loop I, we have now measured the rate of conformational interconversion. This allows us to correlate the process with the pre-steady-state kinetic data on wild-type DHFR and its site-directed mutants to provide insights into the role of the loop in catalysis.

MATERIALS AND METHODS

The wild-type protein was purified and prepared as described previously (Falzone et al., 1990). The pH of the 3 mM sample used for the NMR studies was adjusted to 6.8 in 50 mM phosphate buffer and 100 mM KCl. ^1H NMR NOESY spectra were recorded in 90% ^1H_2O–10% ^2H_2O at 303 K with a Bruker AM-500 spectrometer. The Hahn-echo NOESY experiments were collected with sine modulation in the F1 dimension (Otting et al., 1986) using standard methods (Kumar et al., 1980; Bodenhausen et al., 1984; Davis, 1989). The spectral width was 12 500 Hz in the F2 dimension (4096 complex points) and 6024 Hz in the F1 dimension; TPPI was used for quadrature detection in the t_1 dimension (Drobny et al., 1979; Marion & Wüthrich, 1983), and a total of 460 t_1 experiments were collected for each mixing time with 96 transients per t_1 value. Mixing times (τ_m) were 10, 20, 35, 75, 100, and 140 ms for the build-up curve. The spectra were processed on a SunSparc Station using the program FTNMR (written by Dr. Dennis Hare). After zero-filling, there were 1024 complex points in the F1 dimension. A weak Lorentz-

† Supported by National Institutes of Health Grants GM 36643 to P.E.W. and GM 24129 to S.J.B. C.J.F. was supported in part by a fellowship from Merck Sharp & Dohme.

‡ The Pennsylvania State University.

§ The Scripps Research Institute.

® Abstract published in *Advance ACS Abstracts*, December 15, 1993.

[1] Abbreviations: DHFR, dihydrofolate reductase; DL1, DHFR loop I mutant; H_2F, 7,8-dihydrofolate; H_4F, 5,6,7,8-tetrahydrofolate; MTX, methotrexate; NMR, nuclear magnetic resonance; NOESY, two-dimensional proton nuclear Overhauser spectroscopy; 2QF-COSY, double-quantum-filtered COSY; ROESY, rotating-frame Overhauser enhancement spectroscopy; TPPI, time proportional phase incrementation.

0006-2960/94/0433-439$04.50/0

to-Gaussian window function was used to process the free induction decays. This window function provided good line shapes without negative intensity. The spectra were referenced to the $^1H^2HO$ resonance at 4.73 ppm.

Data Analysis. The rate of exchange was evaluated by measuring cross-peak volumes as a function of mixing time and fitting to the equations of Jeener et al. (1979) for a reversible two-site exchange. The process is represented by

$$A \underset{k_r}{\overset{k_f}{\rightleftharpoons}} B \quad (1)$$

and the volume of the cross-peak connecting form A and form B (a_{AB}) is given by

$$a_{AB}(\tau_m) = a_{BA}(\tau_m) \propto \exp[-(\rho + k)\tau_m] \sinh(k\tau_m) \quad (2)$$

where ρ is the intrinsic spin–lattice relaxation rate, assumed to be equal in form A and form B, and k is the average rate constant for the process, i.e., $(k_f + k_r)/2$. The population of each isomer was assumed to be equal. Nonlinear fitting was performed with the SAS package running on an IBM mainframe computer.

RESULTS AND DISCUSSION

The presence of negative cross-peaks in a 40-ms ROESY spectrum (Li et al., 1992) shows that several protons of wild-type apo-DHFR sample two or more environments slowly on the NMR time scale at room temperature. This phenomenon is not observed in complexes of MTX or folate with DHFR. Exchange cross-peaks are readily distinguished from NOESY cross-peaks in the rotating-frame experiment: exchange cross-peaks and the diagonal have negative intensity whereas rotating-frame NOEs are positive (Bothner-By et al., 1984). Several of the protons participating in chemical exchange can be assigned, but owing to broad lines, significant spectral overlap, and the limited ability to trace NOEs from doubled resonances, the number of ^1H assignments for residues associated with this slow exchange process is severely limited. Thus, there are at least four unassigned aliphatic resonances between 0 and 1.0 ppm which give rise to exchange cross-peaks in the ROESY spectrum and demonstrate that the phenomenon involves several residues. The resonances for which assignments can be made all arise from residues proximal to loop I. They include Trp-22 $N^\epsilon H$ (10.38, 10.54 ppm), Leu-24 $C^\delta H_3$ (0.14, 0.23 ppm), Ile-115 $C^\gamma H_3$ (0.07, 0.17 ppm), and Ile-115 $C^\delta H_3$ (–0.86, –0.67 ppm). Moreover, when three hairpin turn forming residues within loop I (9–24) are deleted (residues 16–19) and a glycine is inserted in the resultant gap, this slow conformational exchange is no longer observed (Li et al., 1992). If the loop dynamics had been slowed so that exchange cross-peaks were no longer detectable, doubling of some of the loop resonances (e.g., from Met-20 or Trp-22) would be expected (Li et al., 1992). This was not observed. Other possibilities include an accelerated rate which leads to single resonances at an average chemical shift or the stabilization of a single nonexchanging conformation (Li et al., 1992).

Figure 1 shows a superposition of a region of the X-ray crystal structures of the MTX (Bolin et al., 1982) and the folate–NADP$^+$ (Bystroff & Kraut, 1991) complexes. The existence of two different conformations of loop I is clearly evident. It is not known what conformations the loop adopts in the apoprotein as it is disordered in the crystal structure (Bystroff & Kraut, 1991). The two distinct possibilities observed in the presence of inhibitor or cofactor and substrate are one in which the key hydrophobic residue Met-20 points away from the active site (MTX complex) and one where

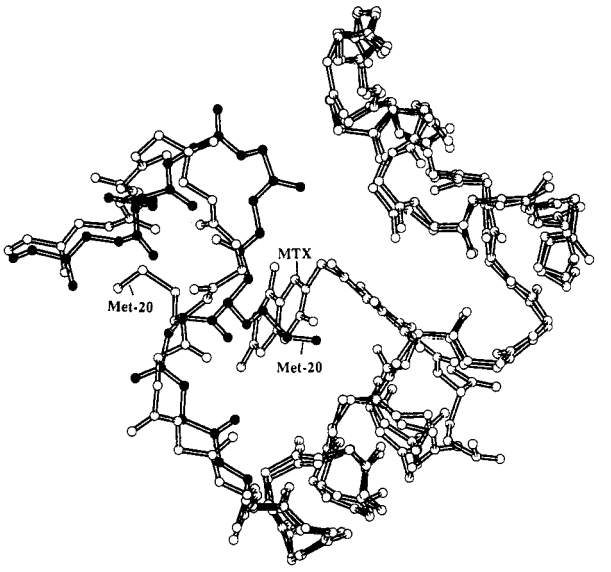

FIGURE 1: Superposition of the X-ray crystal structures for the MTX complex (Bolin et al., 1982) and the ternary folate–NADP$^+$ (Bystroff et al., 1991) complex for residues 12–54. In the ternary complex, the backbone atoms are solid black spheres for residues 13–23, and Met-20 is to the right and overlapping with MTX (folate and NADP$^+$ are not shown for clarity). In the inhibitor complex, atoms are open circles for these residues, and Met-20 is to the left and pointing away from MTX. Note that the backbone atoms are nearly superimposed in most regions except for the atoms associated with loop I.

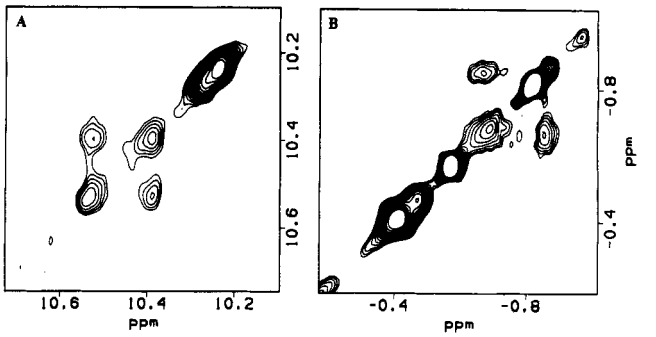

FIGURE 2: (A) Downfield section of a 35-ms NOESY spectrum of wild-type apo-DHFR. The off-diagonal cross-peaks result from the slow exchange of Trp-22 $N^\epsilon H$ between its two environments. It is these cross-peaks that were used in the data analysis. (B) Exchange of Ile-115 $C^\delta H_3$ between two environments in this same NOESY experiment.

Met-20 is directed toward and makes hydrophobic contact with the substrates.

Figure 2 displays two regions of a 35-ms NOESY spectrum where the slow exchange of the $N^\epsilon H$ of Trp-22 (A) and the $C^\delta H_3$ of Ile-115 (B) between two environments is detected. As observed in other forms (Falzone et al., 1990), Ile-115 is in dipolar contact with Trp-22 and is likely to report on the exchange of this aromatic residue in loop I. The chemical shift difference between $N^\epsilon H$ of Trp-22 in its two environments is 77 Hz, a value which places an upper limit of approximately 140 s^{-1} (Sandström, 1982) on the exchange rate for this residue. The chemical shift difference for another residue, Leu-24 [Figure 3 of Li et al. (1992)], places this limit at about 50 s^{-1}. In order to evaluate the rate of the process, the volumes of selected exchange cross-peaks were measured in a series of variable mixing time NOESY experiments. Those for $C^\delta H_3$ of Ile-115 were too broad to provide accurate volumes whereas cross-peaks for Trp-22 $N^\epsilon H$, although broad, are almost completely resolved at 10.38 and 10.54 ppm and were chosen for the analysis. Figure 3 shows volumes (in arbitrary units)

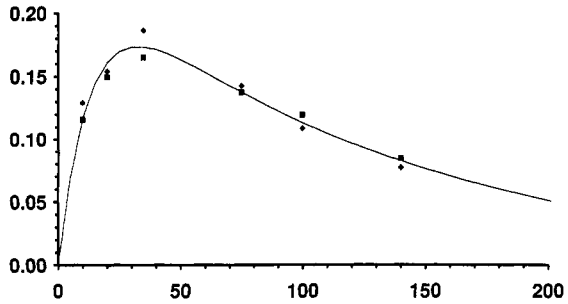

FIGURE 3: Plot of cross-peak volume vs mixing time for the exchange of N$^{\epsilon}$H of Trp-22 between two environments. The curve represents a best fit to these data generated using eq 2 and corresponds to an average first-order rate of 35 s^{-1}. NOESY spectra with mixing times of 10, 20, 35, 75, 100, and 140 ms were used in this analysis.

versus mixing time for these cross-peaks. The corresponding diagonal peaks were not used for quantitative purposes because of extraneous intensity contributions. A best fit of the cross-peak data according to eq 2 gives an average exchange rate of 35 s^{-1}; the curve generated for this rate is depicted in Figure 3. The structural differences between the two forms cannot be determined by using ^{1}H NMR methods because of the complex spectra associated with the apoprotein.

Loop I dynamics in the apoprotein reflect the intrinsic flexibility of an element of secondary structure with its potential for involvement in the catalytic mechanism of DHFR. We hypothesize that the "natural" frequency of loop movement in the apoprotein represents a basal rate for the loop dynamics within the binary or ternary complexes. Studies on the DL1 mutant, which owing to the residue deletions has its loop in an open position (Li et al., 1992), indicate that loop I contributes significantly to the rate enhancement of hydride transfer, given the 500-fold reduction in the chemical step of hydride transfer observed with this mutant. Furthermore, values for the off-rate of H_4F from the free enzyme or the NADPH complexes for the DL1 mutant are 8 and 10 s^{-1}, respectively (Li et al., 1992), compared to the wild-type values of 1 and 12 s^{-1} (Fierke et al., 1987). Thus, the binding synergism where NADPH binding promotes product release, an essential feature of the wild-type mechanism, is largely absent, suggesting that the binding of NADPH to E–H_4F may promote loop opening (Li et al., 1992). In addition, the off-rates for NADPH from the E–NADPH complex and for $NADP^+$ from the E–$NADP^+$–H_4F complex are increased from 4 to 185 s^{-1} and from 200 to 437 s^{-1} when the wild-type enzyme is compared to the DL1 mutant. We view off-rates of 10–12 s^{-1} as characteristic of H_4F dissociation from a conformation in which the loop is in an open position in contrast to the closed-loop position in the ternary $NADP^+$–folate complex. Similarly, off-rates of 4 s^{-1} should be associated with the escape of NADPH from the binary cofactor complex and may also temporarily require the loop in the open position given the large effect of the loop deletion. As observed in the X-ray crystal structure of the ternary complex, the closed position has a hydrogen bond between the Asn-18 side chain and the backbone of His-45 which effectively seals the active site. If the rate constant for loop movement in E–NADPH or E–NADPH–H_4F is only 3-fold slower than in the apoprotein (recall no movement is seen for the E–MTX or E–folate complexes), it would enter into the observed off-rate ($1/k_{off} = 1/k_{loop} + 1/k_{diss}$) where k_{loop} and k_{diss} define rate constants for loop movements from the closed to the open position and the dissociation of H_4F and NADPH from their respective complexes.

In a similar fashion, mutation of a residue essential for proper closure of an active-site loop in triosephosphate isomerase resulted in a 2000-fold drop in the catalytic activity (k_{cat}/K_M) (Sampson & Knowles, 1992a,b). The catalytic activity of this mutant in turn exhibited sensitivity to the viscosity of the medium and showed a large primary isotope effect, suggesting that loop closure and substrate deprotonation are coupled and most likely occur in the same rate-limiting step (Sampson & Knowles, 1992a,b). The inference from these data is that the native isomerase has loop movement tied to a proton-transfer step, although this step, unlike the loss of H_4F from DHFR, is only partially rate-limiting. However, one cannot deduce from the nature of the data whether the rate of loop movement is a major component of this proton abstraction step in the native isomerase enzyme.

The effect that mutations in the αC helix have on the ability of NADPH to trigger H_4F (product) release also implicates loop I movement as a contributor to the off-rate for H_4F. For example, R44L shows a greater dependence on the substrate-assisted product release than is observed in the wild-type protein (Adams et al., 1989) whereas L54I (proximal to αC) has largely removed this effect (Murphy & Benkovic, 1988). Owing to the hydrogen bond between this α-helix and loop I in the ternary complex, mutations in or near the αC helix may enhance or diminish loop I interactions in its closed form and thus may directly affect the need for NADPH binding in product release. In other words, these mutations across the active site may be stabilizing or destabilizing the closed form of the loop.

DHFR has presented an opportunity to examine the dynamics of an element of secondary structure instrumental in achieving high substrate turnover. Our data suggest that the enzyme functions within the limitations set by the loop conformational change in order to improve catalysis through a mobile structural unit rather than crowding the active site with rigid hydrophobic residues which may lack the proper molecular motions to stabilize the transition state (Benkovic et al., 1988; Li et al., 1992; Farnum et al., 1991). These correlations between structural dynamics and microscopic rate constants must be explored in order to elucidate fully the mechanisms by which enzymes enhance the rates of their reactions.

REFERENCES

Adams, J., Johnson, K., Matthews, R., & Benkovic, S. J. (1989) *Biochemistry 28*, 6611–6618.
Adams, J. A., Fierke, C. A., & Benkovic, S. J. (1991) *Biochemistry 30*, 11046–11054.
Appleman, J. R., Howell, E. E., Kraut, J., & Blakley, R. L. (1990) *J. Biol. Chem. 265*, 5579–5584.
Benkovic, S. J., Fierke, C. A., & Naylor, A. M. (1988) *Science (Washington, D.C.) 239*, 1105–1110.
Bodenhausen, G., Kogler, H., & Ernst, R. R. (1984) *J. Magn. Reson. 58*, 370–388.
Bolin, J. T., Filman, D. J., Matthews, D. A., Hamlin, R. C., & Kraut, J. (1982) *J. Biol. Chem. 257*, 13650–13662.
Bothner-By, A. A., Stephens, R. L., Lee, J., Warren, C. D., & Jeanloz, R. W. (1984) *J. Am. Chem. Soc. 106*, 811–813.
Bystroff, C., & Kraut, J. (1991) *Biochemistry 30*, 2227–2239.
Bystroff, C., Oatley, S. J., & Kraut, J. (1990) *Biochemistry 29*, 3263–3277.
Cayley, P. J., Dunn, S. M. J., & King, R. W. (1981) *Biochemistry 20*, 874–879.
Davis, D. G. (1989) *J. Magn. Reson. 81*, 603–607.
Drobny, G., Pines, A., Sinton, S., Weitekamp, D. P., & Wemmer, D. (1979) *Symp. Faraday Soc. 13*, 49–55.
Falzone, C. J., Benkovic, S. J., & Wright, P. E. (1990) *Biochemistry 29*, 9667–9677.
Falzone, C. J., Wright, P. E., & Benkovic, S. J. (1991) *Biochemistry 30*, 2184–2191.

Farnum, M. F., Magde, D., Howell, E. E., Hirai, J. T., Warren, M. S., Grimsley, J. K., & Kraut, J. (1991) *Biochemistry 30*, 11567–11579.
Fierke, C. A., Johnson, K. A., & Benkovic, S. J. (1987) *Biochemistry 26*, 4085–4092.
Hershlag, D. (1988) *Bioorg. Chem. 16*, 62–96.
Jeener, J., Meier, B. H., Bachmann, P., & Ernst, R. R. (1979) *J. Chem. Phys. 71*, 4546–4553.
Kumar, A., Ernst, R. R., & Wüthrich, K. (1980) *Biochem. Biophys. Res. Commun. 95*, 1–6.
Li, L., Falzone, C. J., Wright, P. E., & Benkovic, S. J. (1992) *Biochemistry 31*, 7826–7833.
Marion, D., & Wüthrich, K. (1983) *Biochem. Biophys. Res. Commun. 113*, 967–974.
Murphy, D. J., & Benkovic, S. J. (1989) *Biochemistry 28*, 3025–3031.
Otting, G., Widmer, H., Wagner, G., & Wüthrich, K. (1986) *J. Magn. Reson. 66*, 187–193.
Sampson, N. S., & Knowles, J. R. (1992a) *Biochemistry 31*, 8482–8487.
Sampson, N. S., & Knowles, J. R. (1992b) *Biochemistry 31*, 8488–8494.
Sandström, J. (1982) *Dynamic NMR Spectroscopy*, Academic Press, New York.